Proceeding Paper

Petrophysical Characteristics of Hydrothermally Altered Volcaniclastic-Rich Sedimentary Sequence on the Naturaliste Plateau, Offshore Southwestern Australia (IODP Site U1513) †

Eun Young Lee [1,*] , Laurent Riquier [2], Maria Luisa G. Tejada [3], Seung Soo Chun [4], Lloyd T. White [5], Bernhard Schnetger [6] and Hans-Jürgen Brumsack [6]

1   Department of Geology, University of Vienna, 1090 Vienna, Austria
2   Institut des Sciences de la Terre de Paris (ISTeP), Sorbonne University, 75005 Paris, France; laurent.riquier@sorbonne-universite.fr
3   Institute for Marine Geodynamics (IMG), Japan Agency for Marine-Earth Science and Technology (JAMSTEC), Yokosuka 237-0061, Kanagawa, Japan; mtejada@jamstec.go.jp
4   Faculty of Earth Systems and Environmental Sciences, Chonnam National University, Gwangju 61186, Republic of Korea; sschun@chonnam.ac.kr
5   GeoQuEST Research Centre, School of Earth, Atmospheric and Life Sciences, University of Wollongong, Wollongong, NSW 2522, Australia; lloydw@uow.edu.au
6   Institute for Chemistry and Biology of the Marine Environment (ICBM), University of Oldenburg, 26129 Oldenburg, Germany; bernhard.schnetger@uni-oldenburg.de (B.S.); hans.juergen.brumsack@uni-oldenburg.de (H.-J.B.)
*   Correspondence: eun.lee@univie.ac.at
†   Presented at the 4th International Electronic Conference on Geosciences, 1–15 December 2022; Available online: https://sciforum.net/event/IECG2022.
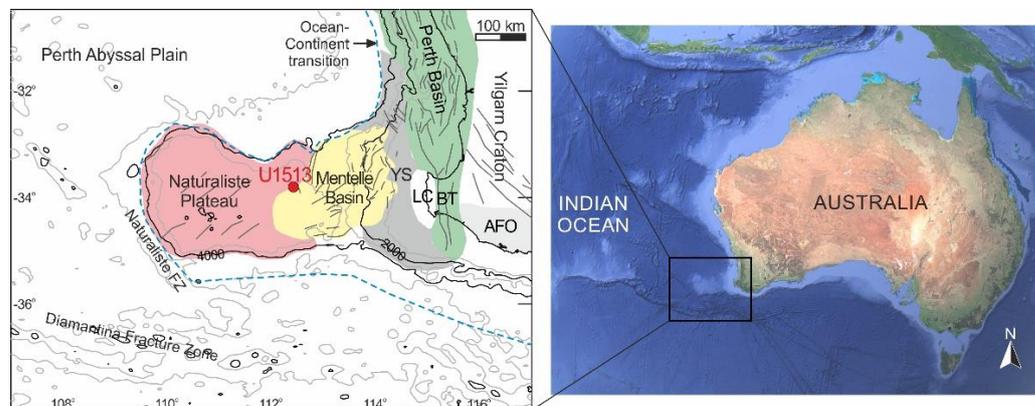
Abstract: Drilling at Site U1513 recovered the Lower Cretaceous volcaniclastic-rich sedimentary sequence on the Naturaliste Plateau and Mentelle Basin, offshore southwestern Australia. The sequence exhibits distinct lithologic characteristics, which are attributed to volcanism and subsidence that occurred during the breakup between Greater India and Australia–Antarctica. It consists of sandstones, siltstones, and silty claystones with abundant volcanic clasts, lithics, and hydrothermal alteration. This study characterizes petrophysical properties of the sequence and correlate them with lithologic and mineralogical features. The properties show noticeable variations. Our results confirm that the petrophysical characteristics are associated with grain size, volcanic matter, organic content, as well as hydrothermal alteration minerals.

Keywords: volcaniclastic-rich sequence; IODP Site U1513; petrophysical properties; hydrothermal alteration; calcite cementation; Naturaliste Plateau; Mentelle Basin; southwest Australia; East Gondwana breakup; Early Cretaceous

1. Introduction

The Naturaliste Plateau is a large submarine continental block (90,000 km^2) in water depths of 2000–5000 m [1]. Along with the Mentelle Basin, Yallingup Shelf, and Perth Basin, this plateau is a part of the southwest Australian rifted continental margin (Figure 1), which formed during the final stages of East Gondwana breakup [2–4]. During International Ocean Discovery Program (IODP) Expedition 369 in 2017, drilling at Site U1513 on the eastern flank of the Naturaliste Plateau and the western margin of the Mentelle Basin (Figure 1) recovered a succession of Cretaceous strata from the late Valanginian to the Campanian [5]. It contains the first in-situ volcanic rocks and a complete sequence of volcaniclastic-rich sedimentary rocks (the Hauterivian to the early Aptian), which spans the transition from the syn- to post-rift phase during the rifting and breakup between Greater India and Australia–Antarctica. Refs. [6–9] described hydrothermal alterations

throughout the volcanic and volcaniclastic-rich sequences. Ref. [3] confirmed that the Naturaliste Plateau subsided from subaerial setting to mid-lower bathyal depths during the Early Cretaceous. The lithologic, mineralogical, and petrophysical characteristics of the lower Cretaceous sequences are associated with the hydrothermal activity and subsidence.
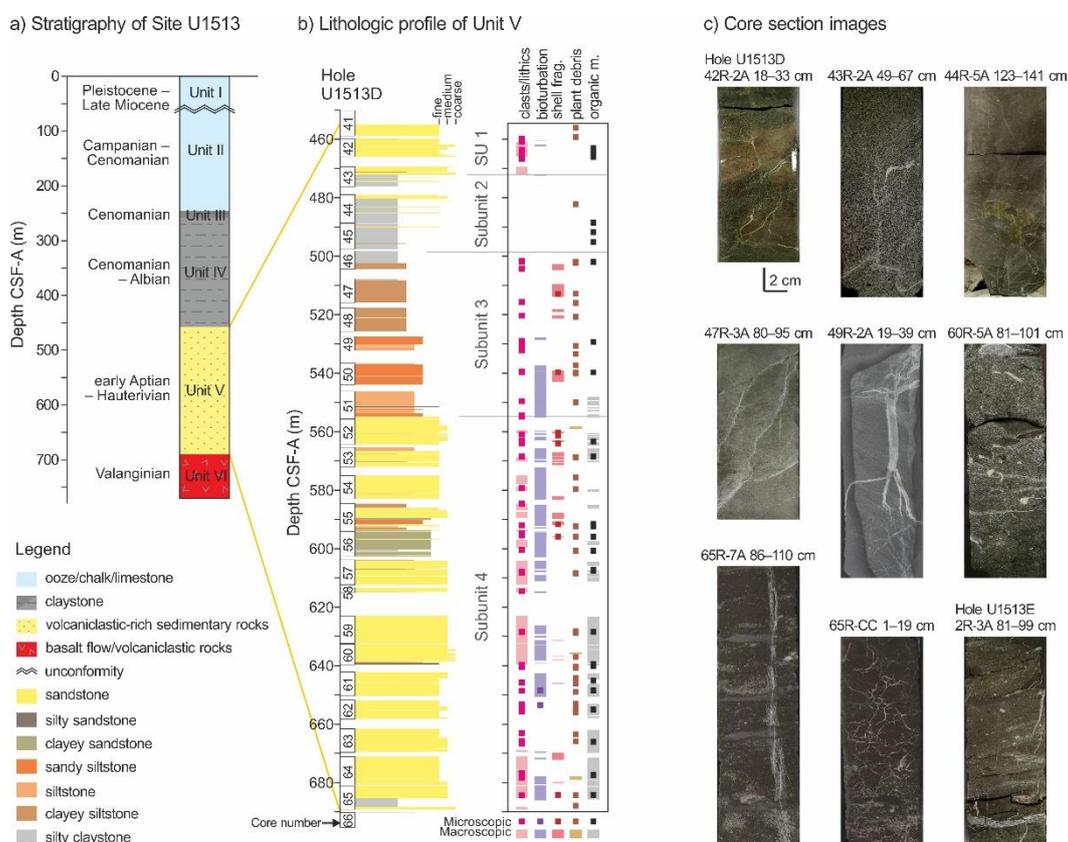

Figure 1. Structural setting of the southwestern Australian rifted margin and adjacent regions in the southeast Indian Ocean: Naturaliste Plateau, Mentelle Basin, Perth Abyssal Plain, Perth Basin, Yilgarn Craton, Yallingup Shelf (YS), Leeuwin Complex (LC), Bunbury Trough (BT), and Albany–Fraser Orogen (AFO). Location of IODP Site U1513 on the eastern flank of Naturaliste Plateau is shown. Thin gray lines show bathymetry (contour interval = 1000 m). Blue dashed line indicates the ocean–continental transition (revised from [4]).

Petrophysical properties are associated with the characterization of the rocks and contained fluids, which are established mainly by lithology, mineral composition, pore network, and fluid [10]. Previous studies reported the effects of primary and post-depositional processes, including compaction, diagenesis, and hydrothermal alteration, on petrophysical properties of volcanogenic rocks (e.g., [11,12]). Ref. [7] investigated petrophysical properties of the volcanic sequence at Site U1513, which exhibited distinct variations that showed a good correlation with primary lithologic characteristics and secondary mineralogical and textural changes attributed to weathering and hydrothermal alteration processes. We suppose that the correlations can be investigated at the overlying volcaniclastic-rich sedimentary sequence at Site U1513, which shows distinct lithologic changes with subsidence and hydrothermal activity [3,9]. In this study, we analyze the petrophysical data of the sequence, including bulk density, grain density, porosity, *P*-wave velocity, thermal conductivity, Natural Gamma Ray (NGR), and magnetic susceptibility data. The data are compared to lithologic descriptions and the mineralogical composition of the section.

2. Materials and Methods

At Site U1513, the 235.33-meter-thick volcaniclastic-rich sedimentary sequence (Lithostratigraphic Unit V; Figure 2a) were recovered at Hole D and Hole E [5]. In Hole D, Unit V was recovered at depths between 454.92 and 690.25 m CSF-A (core depth below seafloor, Method A) (interval 41R-4, 90 cm, through 66R-1, 8 cm) (Figure 2b). In Hole E, Unit V was recovered at depths between 685.2 and 688.07 m CSF-A (interval 2R-1, 0 cm, through 2R-3, 100 cm). Aboard the ship and at the Kochi Core Center (KCC, Kochi, Japan), the core sections were described at the macroscopic and microscopic scales, which include lithology, mineralogical composition, grain size, sedimentary structure, paleontological observations, faults, and hydrothermal veins. The descriptions were combined with mineral identification from whole-rock X-ray diffraction (XRD) data [3,5,13]. During the expedition, petrophysical properties were measured on the whole-round, archive-half and working-half core sections, and discrete core samples (see [13] for instruments and analytical methods). Whole-round core sections were used to estimate bulk density via Gamma Ray Attenuation (GRA) and measure NGR. GRA bulk density data measured at void or fractured intervals

were not considered in this study (usually <1.5 g/cm^3). NGR spectral data were processed to estimate K, Th, and U abundance following the process described by [14]. After splitting cores lengthwise into archive- and working-half sections, the archive-half sections were used to measure point magnetic susceptibility. The working-half sections were selected to measure *P*-wave velocity and thermal conductivity. A total of 56 discrete samples were collected from the working-half sections to determine grain density, bulk density, and porosity using the Moisture and Density (MAD) analysis. After the expedition, 5 discrete samples were selected for the additional MAD analysis, which was reported in [15]. The selected core sections and samples were taken from what were deemed the most suitable and representative lithologic components of the cores, as well as from the least fractured sections.

Figure 2. (**a**) Stratigraphy of IODP Site U1513 with Lithostratigraphic Units I to VI and geologic age [5]. (**b**) Lithologic profile of the volcaniclastic-rich sedimentary sequence (Unit V) at Hole U1513D with subunits 1–4, core numbers, and macroscopic and microscopic observations. Distributions of volcanic clasts, lithic fragments, bioturbation, shell fragments, plant debris, and unidentified organic matter are shown [3]. (**c**) Section images of Unit V showing distinct features including hydrothermal veins, calcite cementation, pyrite nodules, bioturbation, shell fragments, and fractures. Section information (core-section, interval) of each image is shown.
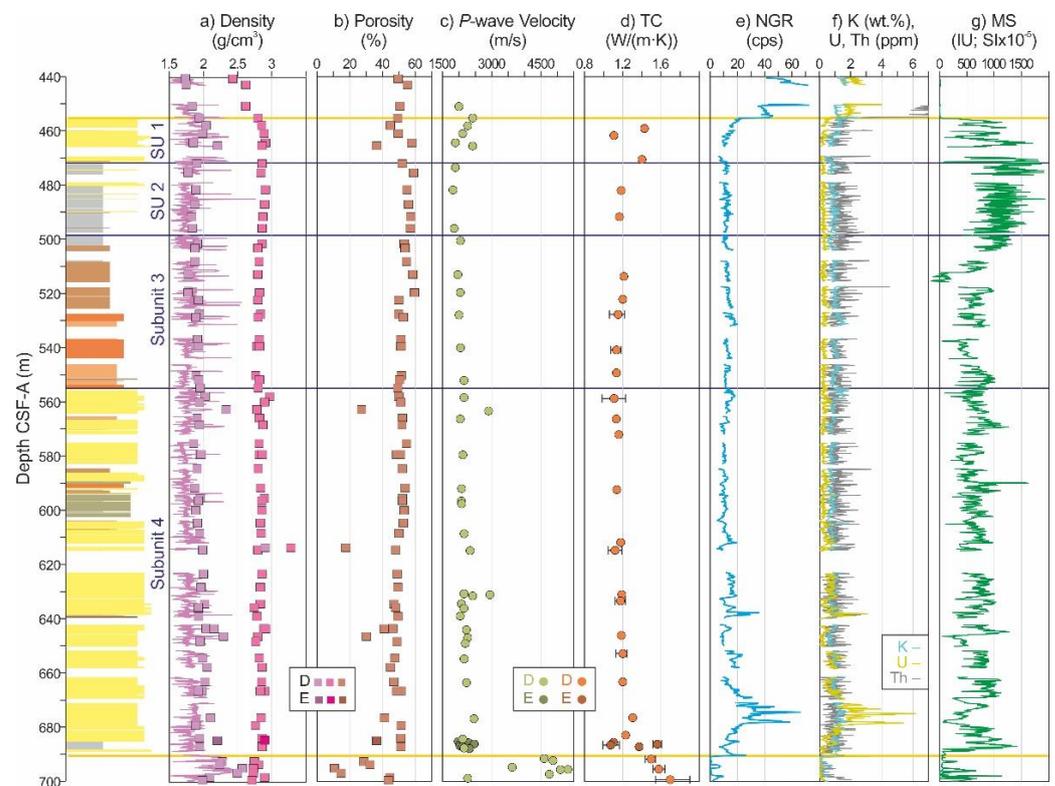
3. Results

3.1. Lithology and Mineralogy

Unit V, i.e., the volcaniclastic-rich sedimentary sequence at Site U1513, is subdivided into four subunits 1–4 (Figure 2b). Major lithology of subunit 4 is massive deposits of coarse- to fine-grained sandstones, subunit 3 consists of massive deposits of siltstones and silty claystones, subunit 2 corresponds to silty claystones with parallel laminations, and subunit 1 consists of massive or laminated layers of coarse- to fine-grained sandstones. Based on microscopic observations and XRD analysis, Ca and Na-rich feldspar (e.g., labradorite), montmorillonite, and chlorite are dominant in subunits 1, 3, and 4, while kaolinite is

dominant in subunit 2 [3]. The volcanic clasts and lithic fragments are present throughout the sequence, being particularly abundant in subunit 4. Bioturbation, shell fragments, and organic matter, including plant debris and unidentified matter, are common in subunits 4 and 3, while being sparse in subunits 2 and 1 (Figure 2b). Hydrothermal alteration is evident from veins observed throughout Unit V. Intervals with intense veining are described in subunit 4 (Figure 2c). Pyrite nodules are present throughout Unit V, while carbonate and siderite nodules are mostly described in subunit 3. Calcite is filling inclined- and irregular-shaped veins with minor fault offsets and slickensides [3,9].

3.2. Petrophysical Properties

Figure 3 presents the petrophysical properties of Unit V: (a) bulk density and grain density; (b) porosity; (c) *P*-wave velocity; (d) thermal conductivity; (e) NGR, (f) K, Th, and U abundance estimated from NGR; and (g) magnetic susceptibility.

Figure 3. Petrophysical properties data acquired from core sections and discrete samples at Hole D (440–700 m CSF-A) and Hole E (685–688 m CSF-A). Section of volcaniclastic-rich sequence (Unit V) is indicated by unit boundaries, subunits 1–4, and lithologic profile [3]. (**a**) Bulk density (g/cm³; purple line and square) and grain density (g/cm³; pink square). Purple line shows bulk density measured using GRA. (**b**) Porosity (%). (**c**) *P*-wave velocity (m/s). (**d**) Thermal conductivity (TC; W/(m·K)). Averaged values are shown (orange dot). (**e**) NGR spectral data (counts per second; cps) and (**f**) estimated abundance of K (wt.%), Th (ppm), and U (ppm). (**g**) Magnetic susceptibility (MS) data. Instrument unit (IU) was converted to dimensionless Système International (SI) unit [16].

In Unit V, bulk density values of MAD data are scattered between 1.76 and 232 g/cm³, being 1.96 g/cm³ on average (Figure 3a). Subunit 4 shows higher bulk density near 2.0 g/cm³ with a few high values of >2.2 g/cm³, while subunits 2 and 3 are 1.85 g/cm³ and 1.87 g/cm³ on average, respectively. Bulk density values from GRA data are generally lower than that of MAD, which is likely due to a gap between the core section and the liner. However, high peaks of GRA bulk density (up to 2.77 g/cm³) are observed throughout the section and are more frequent in subunit 3. Grain density oscillates between 2.74 and 2.96 g/cm³ with 2.85 g/cm³ on average (Figure 3a). Subunit 3 shows lower grain density

with 2.81 g/cm^3, while other subunits show 2.86 g/cm^3. One distinct outlier at ~614 m CSF-A was recorded with 2.88 g/cm^3 in bulk density and 3.28 g/cm^3 in grain density.

Porosity is scattered between 17% and 59%; however, it is generally near 49% (Figure 3b). Several samples show lower values than 40% (the abovementioned outlier is 17.7%), which are described at subunits 1 and 4. Higher porosity values are recorded in subunit 2, being 55.5% on average.

P-wave velocity ranges from 1790 to 2936 m/s with 2157 m/s on average (Figure 3c). The bottom of Unit V is marked by a sharp drop of *P*-wave velocity from 4573 to 2118 m/s. Lower values near 1800 m/s are recorded in subunit 2, while higher values near 2900 m/s are marked in subunit 4.

Thermal conductivity ranges from 1.08 to 1.57 W/(m·K) with 1.19 W/(m·K) on average (Figure 3d). Thermal conductivity remains relatively stable in the section, except near the bottom and top. The highest and lowest values are recorded at 686.3 and 686.7 m CSF-A of Hole E, which is near a contact with an altered basalt flow.

NGR is 12.8 cps, on average, and less than 20 cps downhole from 455 to 637 m CSF-A (Figure 3e). It increases at ~638, ~653, ~685, ~690 m, and between 666 and 682 m CSF-A up to 66.7 cps in the lower section of subunit 4. K concentrations, estimated using NGR, remain quite stable near 1 wt%, while Th concentrations display high peaks up to 4.5 ppm in subunit 3 and U concentrations increase to 6.2 ppm in the lower section of subunit 4, corresponding to the highest values of the NGR (Figure 3f).

The top of Unit V at 454.92 m CSF-A is characterized by a sharp rise in magnetic susceptibility, which is 752 IU, on average, with high variance up to 1941 IU (Figure 3g). Magnetic susceptibility in subunit 2 exhibits higher values with 1150 IU on average, while the values in subunits 3 and 4 are variable but lower, being ~668 IU and ~686 IU on average.

4. Discussion

The four subunits of Unit V exhibit different lithologic characteristics, which we attribute to changes in grain size, mineral components, and abundance of volcanic clasts, lithics, and organic matter (Figure 2b). Hydrothermal features, including calcite vein/cementation and nodule occurrence, are described throughout the section, and are distinct in certain intervals. The characteristics of each subunit are related to variations in the petrophysical properties, as observed in Figure 3.

Subunit 4 displays higher bulk density, lower porosity, and higher *P*-wave velocity compared to those in other subunits, which are distinctly noticeable in several intervals (Figure 3a–c). These trends are associated with abundant high-density materials (volcanic clasts, lithics, and pyrites), calcite veins, and cementation. Occasionally, high GRA bulk density could be related to presence of calcite cementation and pyrite nodules (pyrite density ~5 g/cm^3). Thermal conductivity shows variable values at the bottom of subunit 4 (Figure 3d), which is described at an interval showing intense hydrothermal activity near the altered basalt flow (Figure 2c). This finding indicates that the thermal conductivity variations correspond to hydrothermal alteration and associated changes [7]. The lower section of subunit 4 includes intervals of higher NGR with higher U concentrations (Figure 3e,f). Since U content is often hosted in organic matter, which is different from K and Th hosting in clay minerals [14], the higher NGR could be attributed to abundant organic matter in the intervals.

Subunits 2 and 3 show relatively stable petrophysical properties, except for magnetic susceptibility (Figure 3). In subunit 2, the lower bulk density, higher porosity, and lower *P*-wave velocity can be related to the porous nature of clays with kaolinite. The stable properties can be related to decreased abundance of volcanic clasts, lithics, and organic matter content compared to subunit 4 (Figure 2b). However, since calcite vein/cementation and nodules are described in the subunits, the properties might result from biased measurements and sampling to select representative lithologic components of the cores. Frequent high peaks in GRA bulk density support the presence of cementation, pyrite, and siderite nodules (siderite density ~3.96 g/cm^3) (Figure 3a). In the variable magnetic susceptibility,

values near 0 IU correspond to intervals showing calcite cementation. The high magnetic susceptibility of subunit 2 is likely associated with the fine grain size [17]. Subunit 1 displays variable lithologic characteristics related to grain size, mineral composition, volcanic clasts, lithics, irregular calcite veins with cementation, pyrites, and sedimentary structure. These characteristics caused variations in bulk density, porosity, thermal conductivity, and magnetic susceptibility.

5. Conclusions

This study describes the lithologic characteristics and petrophysical properties of 235-meter-thick volcaniclastic-rich sedimentary rocks (Unit V) at Site U1513 on the eastern Naturaliste Plateau. Subunits 1–4 exhibit different lithologic features, with these differences attributed to changes in grain size, mineral composition, abundance of volcanic clasts, lithics, organic matter, and hydrothermal alteration features. These trends are correlated with petrophysical trends and variations. Subunit 4 displays lower values of porosity and higher values of bulk density and P-wave velocity, which correspond to abundant high-density materials and alteration contents. Higher NGR intervals are attributed to abundant organic matter content. In subunits 3 and 2, the petrophysical properties remain relatively stable, except magnetic susceptibility. The higher porosity and lower bulk density and P-wave velocity in subunit 2 correspond to the porous clays with kaolinite. The magnetic susceptibility is highly variable throughout the sequence with mineral composition and grain size. Variations in thermal conductivity in subunits 4 and 1 correspond to intervals showing hydrothermal alteration. We conclude that the petrophysical properties and their distinct variations in Unit V are associated mainly with primary lithologic characteristics, as well as secondary mineralization formed by hydrothermal activity.

Institutional Review Board Statement: Not applicable.

Informed Consent Statement: Not applicable.

Data Availability Statement: Data presented in this manuscript can be accessed via the data repository of IODP (http://web.iodp.tamu.edu/LORE/) and found in IODP data report (Lee and Song, 2021).

Conflicts of Interest: The authors declare no conflict of interest.

References

1. Borissova, I. *Geological Framework of the Naturaliste Plateau, Record 2002/20*; Geoscience Australia: Canberra, Australia, 2002.
2. Gibbons, A.D.; Whittaker, J.M.; Muller, R.D. The breakup of East Gondwana: Assimilating constraints from Cretaceous ocean basins around India into a best-fit tectonic model. *J. Geophys. Res. Solid Earth* **2013**, *118*, 808–822. [CrossRef]
3. Lee, E.Y.; Wolfgring, E.; Tejada, M.L.G.; Harry, D.L.; Wainman, C.C.; Chun, S.S.; Schnetger, B.; Brumsack, H.-J.; Maritati, A.; Martinez, M.; et al. IODP Expedition 369 Science Party, Early Cretaceous subsidence of the Naturaliste Plateau defined by a new record of volcaniclastic-rich sequence at IODP Site U1513. *Gondwana Res.* **2020**, *82*, 1–11. [CrossRef]
4. Harry, D.L.; Tejada, M.L.G.; Lee, E.Y.; Wolfgring, E.; Wainman, C.C.; Brumsack, H.-J.; Schnetger, B.; Kimura, J.-I.; Riquier, L.; Borissova, I.; et al. Evolution of the southwest Australian rifted continental margin during breakup of East Gondwana: Results from IODP Expedition 369. *Geochem. Geophy. Geosyst.* **2020**, *21*, e2020GC009144. [CrossRef]

5.   Huber, B.T.; Hobbs, R.W.; Bogus, K.A.; Batenburg, S.J.; Brumsack, H.-J.; do Monte Guerra, R.; Edgar, K.M.; Edvardsen, T.; Harry, D.L.; Hasegawa, T.; et al. Site U1513. In *Australia Cretaceous Climate and Tectonics*; Hobbs, R.W., Huber, B.T., Bogus, K.A., Expedition 369 Scientists, Eds.; IODP: College Station, TX, USA, 2019.

6.   Tejada, M.L.G.; Lee, E.Y.; Chun, S.S.; Harry, D.L.; Riquier, L.; Wainmann, C.C. Data report: Petrology and volcanic stratigraphy at Site U1513, IODP Expedition 369. In *Australia Cretaceous Climate and Tectonics*; Hobbs, R.W., Huber, B.T., Bogus, K.A., Expedition 369 Scientists, Eds.; IODP: College Station, TX, USA, 2020.

7.   Lee, E.Y.; Tejada, M.L.G.; Song, I.; Chun, S.S.; Gier, S.; Riquier, L.; White, L.T.; Schnetger, B.; Brumsack, H.-J.; Jones, M.M.; et al. Petrophysical Property Modifications by Alteration in a Volcanic Sequence at IODP Site U1513, Naturaliste Plateau. *J. Geophys. Res. Solid Earth* **2021**, *126*, e2020JB021061. [CrossRef]

8.   Riquier, L.; Lee, E.Y.; Tejada, M.G.L. Data report: X-ray diffraction mineralogy of a volcanic sequence at Site U1513 (Naturaliste Plateau), IODP Expedition 369. In *Australia Cretaceous Climate and Tectonics*; Hobbs, R.W., Huber, B.T., Bogus, K.A., Expedition 369 Scientists, Eds.; IODP: College Station, TX, USA, 2021.

9.   White, L.T.; Forster, M.A.; Tanner, D.; Tejada, M.L.G.; Hobbs, R.; IODP Expedition 369 Science Party. Age of magmatism and alteration of basaltic rocks cored at the base of IODP Site U1513, Naturaliste Plateau, southwestern Australia. *Aust. J. Earth Sci.* **2022**, *69*, 383–405. [CrossRef]

10. Cannon, S. *Petrophysics: A Practical Guide*; Willey Blackwell: Chichester, UK, 2016; p. 224.

11. Durán, E.L.; Adam, L.; Wallis, I.C.; Barnhoorn, A. Mineral alteration and fracture influence on the elastic properties of volcaniclastic rocks. *J. Geophys. Res. Solid Earth* **2019**, *124*, 4576–4600. [CrossRef]

12. Pola, A.; Crosta, G.; Fusi, N.; Barberini, V.; Norini, G. Influence of alteration on physical properties of volcanic rocks. *Tectonophysics* **2012**, *566–567*, 67–86. [CrossRef]

13. Huber, B.T.; Hobbs, R.W.; Bogus, K.A.; Batenburg, S.J.; Brumsack, H.-J.; do Monte Guerra, R.; Edgar, K.M.; Edvardsen, T.; Harry, D.L.; Hasegawa, T.; et al. Methods. In *Australia Cretaceous Climate and Tectonics*; Hobbs, R.W., Huber, B.T., Bogus, K.A., Expedition 369 Scientists, Eds.; IODP: College Station, TX, USA, 2019.

14. De Vleeschouwer, D.; Dunlea, A.G.; Auer, G.; Anderson, C.H.; Brumsack, H.; de Loach, A.; Gurnis, M.; Huh, Y.; Ishiwa, T.; Jang, K.; et al. Quantifying K, U, and Th contents of marine sediments using shipboard natural gamma radiation spectra measured on DV JOIDES resolution. *Geochem. Geophy. Geosyst.* **2017**, *18*, 1053–1064. [CrossRef]

15. Lee, E.Y.; Song, I. Data report: Moisture and Density (MAD) analysis and Ultrasonic velocity of Hole U1513E, IODP Expedition 369. In *Australia Cretaceous Climate and Tectonics*; Hobbs, R.W., Huber, B.T., Bogus, K.A., Expedition 369 Scientists, Eds.; IODP: College Station, TX, USA, 2021.

16. Searle, R.C. Magnetic susceptibility as a tool for investigating igneous rocks—Experience from IODP Expedition 304. *Sci. Drill.* **2018**, *6*, 52–54. [CrossRef]

17. Dunlop, D.J.; Özdemir, Ö. *Rock Magnetism Fundamentals and Frontiers*; Cambridge University Press: Cambridge, UK, 1997.